Density functional study of Pt_4 clusters adsorbed on a carbon nanotube support

Nguyen Thanh Cuong,[1] Ayumu Sugiyama,[1] Akihiko Fujiwara,[1] Tadaoki Mitani,[2] and Dam Hieu Chi[1,2,3]
[1]*Japan Advanced Institute of Science and Technology, 1-1 Asahidai, Nomi, Ishikawa 923-1292, Japan*
[2]*Shimoda Nano-Liquid Process Project, ERATO, Japan Science and Technology, 2-5-3 Asahidai, Nomi, Ishikawa 923-1211, Japan*
[3]*Hanoi University of Science, 334 Nguyen Trai, Thanh Xuan, Hanoi, Vietnam*
(Received 26 January 2009; revised manuscript received 8 May 2009; published 16 June 2009)

Small clusters on substrates usually exhibit large numbers of configurations separated by relatively small barriers and easily interconvert between such configurations, known as *structural fluxionality*. We investigate here this property in hybrid catalytic structure: small Pt clusters adsorbed on single-wall carbon nanotube (SWNT) support using density functional calculations. We find that the Pt_4 clusters adsorbed on SWNT support exhibit several energetically accessible structural isomers with rather low-energy barriers, resulting in the high degree of structural fluxionality. We find that curvature of SWNT and charge redistribution play important roles in the variation in structure of Pt_4 cluster on SWNT. The high degree of structural fluxionality allows the Pt_4 clusters on SWNT to interact easily with environmental gas molecules such as CO by adapting their structures. The change in electronic structure via molecular adsorption due to the structural fluxionality and the variation in structure caused by changes in electronic structure are strongly interrelated resulting in the wide variety of dynamic reactions of CO molecules with Pt_4 clusters.

DOI: 10.1103/PhysRevB.79.235417 PACS number(s): 68.43.Bc, 61.46.−w, 73.22.−f

I. INTRODUCTION

Platinum metal is widely used in environmentally and economically important processes such as catalytic conversion of harmful gases,[1] hydrogenation, and electrode reactions of fuel cells[2] because of its high catalytic activity. It is, however, a precious metal and quite expensive. Therefore, reduction in the consumption of platinum is one of the most important issues. By enhancing the catalytically active area relative to the volume of platinum by using "small clusters," a significant reduction in consumption is expected. Miniaturization of materials usually results not only in the enhancement of relative surface area, but also in changes in the property itself. As for catalysts, nanometer-scale clusters usually exhibit unique catalytic properties that differ from those of extended flat surface or bulk materials.[3,4] Characterization and precise control of the catalytic properties of nanoclusters are among the outstanding challenges in the research fields of both physics and chemistry.

Nanoclusters usually have several structural isomers with comparable formation energies and each isomer with different surface geometry is expected to show different catalytic activity.[5–8] When the interconversion energy barriers among isomers are low enough, clusters exhibit rapid fluctuation among different isomers namely "a structural fluxionality."[9] Thus, the structural fluxionality can cause dramatic changes in the concentration of active sites and the dynamic geometrical changes due to fluxionality can allow the reactants to overcome reaction barriers by adapting the cluster's structure for a distinctive catalytic reactivity.

The structural stability and fluxionality are also affected by the environmental situation. It is well known that ligands and/or supports are required for the stabilization of nanoclusters.[10] Moreover, interactions between nanoclusters and reactant molecules will modify the electronic structure of the metal clusters and drastically affect the geometry of the nanoclusters. Therefore, investigations of the structural change in metal clusters under the gas environments are needed in order to understand the behavior of nanoclusters and the catalytic reaction processes. This means that the formation energy and geometry are determined not only by the nanocluster itself, but also by the supporting materials and other environmental conditions. Catalytic reactions with nanoclusters should be, therefore, understood in terms of the dynamic structural fluxionality of hybrid systems.

Recently, carbon nanotubes (CNTs), with high surface area, good electronic conductivity, and high chemical stability, have been found to be an ideal support material for Pt clusters.[11] Highly dispersed and size-controlled small Pt clusters (less than 1 nm) made from dispersed single Pt atoms were achieved by using CNT supports.[12] The motion of Pt clusters on CNT was also observed experimentally by high-resolution transmission electron microscopy. In addition, our previous theoretical results indicated that Pt atoms can move easily between adsorption sites on the surface of CNT, although they bind strongly to CNT.[13,14] These findings reveal a high capability to change geometric structure of small Pt clusters on CNT support.

In this paper, we have investigated the geometry and electronic structure of small Pt clusters adsorbed on single-wall carbon nanotube (SWNT) support using first-principles density functional calculations. The tetrahedral Pt_4 clusters on the (10, 0) SWNT is investigated as a model to explore Pt cluster-SWNT catalyst, within a reasonable computational time. We first find that the existence of many energetically possible isomers of Pt cluster indicates that a high degree of structural fluxionality of Pt_4 clusters on SWNT support. Second, we demonstrate that the geometry and electronic structure of isomers of Pt_4 cluster on SWNT are strongly interrelated. Finally, we discuss the structural change in the Pt_4 clusters on SWNT under CO gas environment, which is a realistic condition for catalytic reactions. Here, we find that the adsorption energies of CO molecule are significantly varied, owing to the adapting structure of Pt clusters. It is sug-

gested that structural fluxionality is essential to the catalytic reactions on nanoclusters.

II. METHODOLOGY

All calculations have been performed using density functional theory (DFT) (Refs. 15 and 16) with DMol^3 program.[17] We used the generalized gradient approximation Perdew-Burke-Ernzerhof functional (GGA-PBE) (Ref. 18) to treat the exchange-correlation energy of interacting electrons. The DFT semicore pseudopotential[19] was adopted to describe the valence electrons-core interaction for Pt with 5*s*, 5*p*, 5*d*, and 6*s* valence electrons; all electron treatments were used for C and O. Double valence plus single-polarization orbitals and a real-space cutoff of 4.5 Å were used for all calculations.

We used periodic boundary conditions and an orthorhombic supercell with dimensions $a=27.00$ Å, $b=20.00$ Å, and $c=17.04$ Å, which were all large enough for us to be able to ignore the interaction between the Pt_4 (10, 0) SWNT and its periodic images. The c lattice aligned with the axis of the tube was four times the lattice parameter of unit cell (i.e., $c=4c_0$). Lattice parameter c_0 of the (10, 0) SWNT unit cell was estimated from ideal graphene sheet. Atomic positions of the (10, 0) SWNT unit cell were optimized. Brillouin-zone integrations were performed using $(1\times1\times8)$ k-points mesh within Monkhorst-Pack scheme.[20] The parameters were chosen to ensure that calculated energies are well converged. To check the effect of spin polarization, we carried out spin-unrestricted calculations for Pt_3, Pt_4, and Pt_5 clusters on the SWNT support, but we did not find any magnetic polarization of the these supported Pt clusters in agreement with previous calculations.[21] Hence, we used spin-restricted calculations in this research.

The relaxed structures of the tetrahedral Pt_4 clusters adsorbed on the (10, 0) SWNT have been optimized carefully without any constraint on symmetry. CO molecular adsorption was carried out on various sites of the Pt_4 clusters on SWNT. For all optimized structure calculations, all atoms in system were relaxed until forces were less than 0.002 Ha/Å. Adsorption energy of Pt_4 clusters on the SWNT and adsorption energy of CO on the Pt_4 clusters on SWNT were computed using the expression

$$E_{\text{ads}} = E_A + E_S - E_{AS}, \tag{1}$$

where E_A represents the total energy of A (isolated Pt_4 cluster or isolated CO molecule), E_S represents the total energy of S (SWNT or Pt_4 SWNT), and E_{AS} represents the total energy of AS (Pt_4 SWNT or CO-Pt_4 SWNT). For density of states calculations, we used $1\times1\times32$ k-points mesh to get a resolution of 0.05 eV Gaussian broadening.

III. RESULTS AND DISCUSSION

A. Structural fluxionality of the Pt_4 clusters on SWNT support

1. Structural isomers

We investigated the relaxed structures of tetrahedral Pt_4 clusters adsorbed on (10, 0) SWNT by setting up various initial structures. Figure 1 shows the three representative configuration types of carbon nanotube supported Pt_4 cluster isomers: (i) one Pt atom in contact directly with the nanotube labeled configuration I [Fig. 1(a)], (ii) two Pt atoms in contact directly with the nanotube, configuration II [Fig. 1(b)], and (iii) three Pt atoms in contact directly with the nanotube, configuration III [Fig. 1(c)]. We find that the Pt atoms of Pt cluster are preferably adsorbed on the bridge sites of C-C bonds or top sites of C atoms in agreement with the adsorption of single Pt atom on SWNTs surface.[13,21] Because of the competitive effects between Pt-C interaction and Pt-Pt interaction, the tetrahedral geometry of supported Pt_4 clusters is slightly distorted. The nearest-neighbor Pt-Pt distances in adsorbed Pt_4 clusters vary from 2.58 Å to 3.04 Å compared with 2.64 Å in the free-tetrahedral Pt_4 cluster. Adsorption energies of the Pt_4 clusters on SWNT(E_{ads}) increase from configuration I to configuration III (1.55, 2.07, and 2.31 eV, respectively). In other words, the adsorption energy tends to increase with increasing number of Pt-C bonds. The results imply that the Pt-C bonds play a vital role in the structural stability of Pt clusters on CNT support.

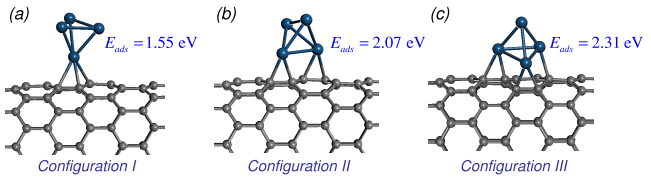

FIG. 1. (Color online) Structures and adsorption energies of the Pt_4 clusters on (10, 0) SWNT. (a) Configuration I: one Pt atom in contact directly with the nanotube, (b) configuration II: two Pt atoms in contact directly with the nanotube, and (c) configuration III: three Pt atoms in contact directly with the nanotube. The light gray balls indicate C atoms and the blue (dark gray) balls indicate Pt atoms.

From more detailed analysis of the effect of Pt-C bonds, we investigated the structural isomers of Pt_4 clusters on SWNT in which the Pt atoms are in contact with the axial C-C bridge site or the zigzag C-C bridge site [Fig. 2(a)]. Figures 2(b)–2(i) show the isomers of three configurations I–III: the most stable isomers for configurations I–III correspond to the structures shown in Fig. 1. We found that the adsorption energies of Pt_4 clusters differ between the isomers in each configuration type. Maximum differences in adsorption energy of isomers for configurations I, II, and III are 0.02, 0.38, and 0.30 eV, respectively. Adsorption energy of Pt cluster on the SWNT is mainly influenced by two opposite contributions: interaction energy of Pt_4 cluster and SWNT (positive) and structural distortion energy of Pt_4 cluster and SWNT (negative). We previously reported that the interaction energy of a single Pt atom on the axial C-C bridge site is greater than that on the zigzag C-C bridge site, 0.12 eV.[13] Distortion energy of Pt_4 clusters (E_{dist}), which is estimated as energy difference between the distorted Pt_4 cluster and the free tetrahedral Pt_4 cluster, is also shown in Fig. 2. The differences of distortion energy among isomers, 0.01–0.21 eV, are smaller than those of adsorption energy, 0.02–0.38 eV. The local-minimum energies of Pt_4 clusters are decided by compensation between binding energy and structural-

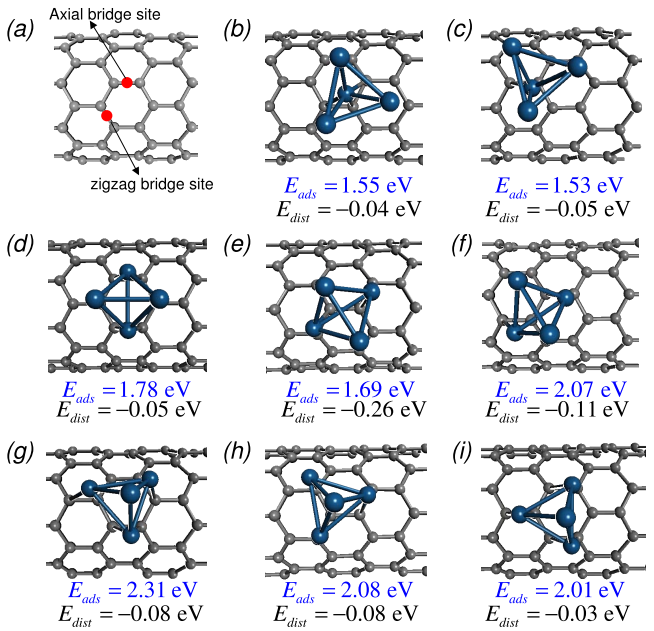

FIG. 2. (Color online) (a) Two types of C-C bridge sites on the (10, 0) SWNT. Top views of structural isomers and adsorption energies, distortion energies of the Pt_4 clusters on (10, 0) SWNT: (b)–(c) configurations I, (d)–(f) configurations II, (g)–(i) configurations III. The light gray balls indicate C atoms and the blue (dark gray) balls indicate Pt atoms.

deformation energy of Pt_4 cluster and SWNT, and the origin of small variation in binding energy among SWNT-supported Pt_4 cluster can be attributed to the offset of these two effects. This result clarified the important roles of curvature and symmetry of SWNT on the structural stability of Pt clusters on CNT support. From the viewpoint of formation energy, our results show that the Pt_4 clusters on SWNT support exhibit large numbers of configurations of comparable energies and hence can result in an interconversion between such isomers.

2. *Interconversion energy barriers*

In order to investigate the capability of the Pt_4 clusters on SWNT support to interconvert between isomers, we estimated the energy barriers among isomers. Considering the symmetry and geometry of the Pt_4 clusters on SWNT, we first focus on interconversions between configuration I [Fig. 2(b)], configuration II [Fig. 2(e)], and configuration III [Fig. 2(h)]. Structures and energy barriers for interconversion pathways between these configurations are shown in Fig. 3. Here, we used linear-synchronous transit and quadratic-synchronous transit methods to search for the transition states (TS).[22] We find that the interconversion of Pt_4 clusters occurs by rolling on the SWNT support. The energy barriers between isomers vary from 0.10 to 1.17 eV. By passing though a transition state (TS1) with a slightly higher barrier of 0.7 eV, one of the upper atoms in Pt_4 cluster of configuration I falls to the surface of SWNT forming configuration II. From this configuration, Pt_4 cluster rotates around the axis formed by the two lower atoms leading to configuration III with a small energy barrier of only 0.1 eV. On the other hand,

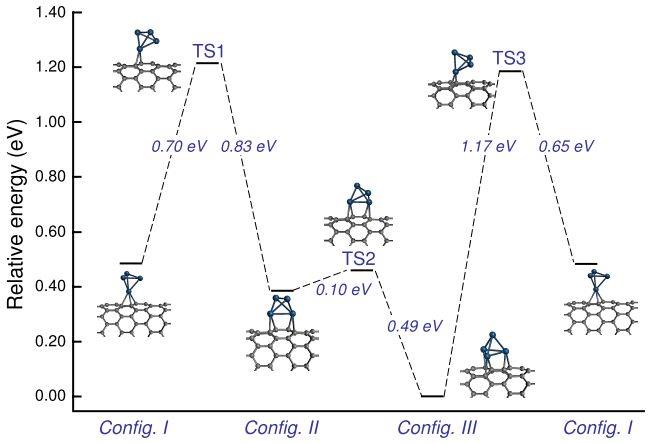

FIG. 3. (Color online) Structures and energy barriers for the interconversion paths between the Pt_4 clusters on (10, 0) SWNT: configuration I [from Fig. 2(b)], configuration II [from Fig. 2(e)], and configuration III [from Fig. 2(h)].

it is difficult to convert directly from configuration III to configuration I because of high-energy barrier of 1.14 eV. The energies required for reverse steps of conversion are different from forward steps because of different adsorption energies among configurations. Second, we also investigated interconversion between isomers of the same configuration type (not shown in figures) and found that energy barriers were as low as ca. 0.2 eV. The relatively small barriers indicate that the Pt_4 clusters adsorbed on the SWNT support can easily interconvert between their isomers at low temperature.

Another issue of interest is the effect of the supporting SWNT's curvature on the interconversion of Pt cluster isomers because the adsorption energy of a single Pt atom or Pt clusters on SWNT strongly depends on the curvature of SWNTs.[13,14,23] To understand the curvature effect, the interconversion pathways and energy barriers of Pt_4 cluster on SWNT support were compared with those of Pt_4 clusters on flat graphene sheet shown in Fig. 4. It is clear from Figs. 3 and 4 that the energy barriers of the Pt_4 clusters on flat graphene sheet are smaller than those on the SWNT support. These low-energy barriers can be attributed to low-adsorption energy of Pt_4 cluster on flat graphene sheet (1.35 eV) compared with that on the (10, 0) SWNT (2.60 eV). The decrease in energy barriers indicates higher capability of Pt

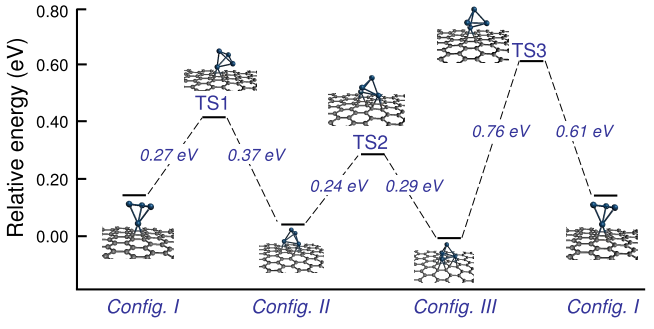

FIG. 4. (Color online) Structures and energy barriers for the interconversion paths between the Pt_4 clusters on flat graphene sheet: configuration I, configuration II, and configuration III.

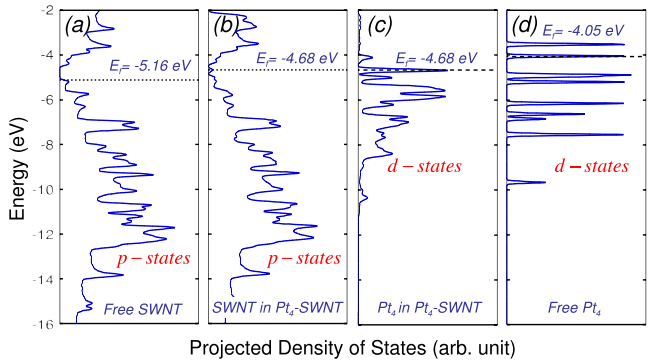

FIG. 5. (Color online) Projected density of states: (a) *p* states of the free (10, 0) SWNT, (b) *p* states of the SWNT in configuration I, (c) *d* states of the Pt_4 cluster in configuration I, and (d) *d* states of the free Pt_4. The horizontal dotted lines denote the Fermi levels.

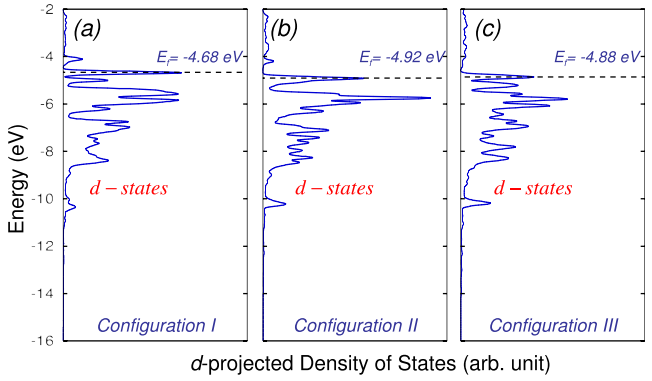

FIG. 6. (Color online) *d*-projected density of states of the Pt_4 clusters in the Pt_4 (10, 0) SWNT: (a) configuration I, (b) configuration II, and (c) configuration III. The horizontal dotted lines denote the Fermi levels.

cluster on flat graphene sheet to interconvert between isomers. Therefore, the curvature of SWNTs plays an important role in the structural fluxionality of small Pt clusters on SWNT support.

Small adsorption energies and barriers of Pt_4 clusters on flat graphene sheet suggest that the Pt_4 cluster are flexible and easily move, and/or coalescence into bigger clusters on the flat surface of graphene sheet at low temperature. Thus, we can predict that it is hard to experimentally achieve small and dispersed Pt clusters on pristine graphene support. The higher-adsorption energies and barriers of the Pt_4 clusters on SWNT support imply that the Pt_4 clusters are rather stable on the surface of SWNT support at low temperature. However, the Pt_4 clusters can move and coalescence into bigger clusters on the surface of pristine SWNT support at the high temperature or catalytic working conditions. These theoretical predictions are consistent with the experimentally observed formation of Pt clusters on CNT support at different high heat temperatures.[12] Practically, in this experimental study, introduction of thiol groups on the surface of a carbon nanotube is indispensable in order to obtain highly dispersed Pt clusters.

B. Interrelation between geometry and electronic structure of the Pt_4 clusters on SWNT support

Electronic structure, which has an important role in physical and chemical properties, is directly related to geometry of clusters on SWNT support. We investigated here density of states and charge-density difference of the three configurations of Pt_4 cluster on SWNT support in the structural interconversion as described in Fig. 3.

We analyzed the *s*, *p*, *d*-projected density of states (PDOS) of the pristine SWNT, the Pt_4-SWNT configurations, and the free Pt_4 cluster. We found that there is a significant change in the *p* states of SWNT and *d* states of Pt_4 cluster. Figure 5 shows *p* PDOS of the SWNT, *d* PDOS of the Pt_4 cluster before and after adsorption for configuration I. There are new hybrid orbitals in a wide range from −8.0 eV to Fermi level indicating a strong hybridization between *p* orbitals of the SWNT and *d* orbitals of Pt cluster. These hybridizations result in the delocalized and broadened of *d* states of the Pt_4 clusters in configurations, as shown in Fig. 6, compared with discrete states of the free Pt_4 cluster [Fig. 5(d)]. However, *d* states of the Pt_4 clusters are involved in both metal-metal interaction and metal-SWNT interaction. The electrons are still confined into and/or around clusters and no longer itinerant as those in the bulk metal, hence the geometrical and electronic properties of the Pt_4 cluster on SWNT support are strongly interrelated. In addition, significant differences in the PDOS at near Fermi level of three configuration types can be observed. The detailed analyses show that *d* states of the C-adjacent Pt atoms are more localized at the Fermi level and broadened in a wide range compared with the Pt atoms combined only with other Pt atoms in the cluster. It is well known that the position and the width of *d* band of transition-metal cluster dictates many of the characteristics of the adsorption of molecules by means of covalent bonding.[24,25] Thus, it can be predicted that various isomers of the Pt_4 cluster on SWNT support exhibit different chemical reactivity.

The distinctive electronic structures of Pt_4 clusters on SWNT among configurations are also characterized by charge-density difference. Figure 7 shows the differences between the charge density of the Pt_4 cluster-SWNT and sum of the charge densities of isolated Pt_4 cluster and of isolated SWNT in three configurations $[\Delta\rho=\rho_{Pt_4-SWNT}-(\rho_{Pt_4}+\rho_{SWNT})]$. Changes in the electron densities occur mainly at interface region between the Pt_4 clusters and the SWNT, where a substantial concentration of electrons accumulates as Pt-C bonds. Table I shows amount of charge transfer from the Pt cluster to the SWNT based on the Hir-

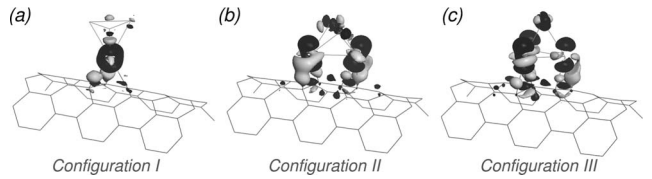

FIG. 7. Charge-density differences in the Pt_4 clusters adsorbed on (10, 0) SWNT: (a) configuration I, (b) configuration II, and (c) configuration III at 0.04 (a.u.) isosurface value. Charge density flows from the dark regions into the light regions.

TABLE I. Charge transfer from the Pt_4 cluster to the (10, 0) SWNT in three configurations based on Hirshfeld analysis.

	Config. I	Config. II	Config. III
Total charge (e)	0.18	0.24	0.24

shfeld charge analysis.[26] Although the difference in the total charge transfer is small, the charge redistributions of Pt atoms within one cluster differ depending on cluster configuration. Moreover, the accumulated charge region can facilitate bonding with electron-acceptor molecules (O_2, CO, etc.).[5,25] Thus, it is expected that the Pt_4 clusters on SWNT support can show a wide variety of catalytic activity.

C. Adsorption of CO molecule on the Pt_4 clusters on SWNT support

CO molecules act both as a catalyst poison and an important reaction intermediate in many processes such as direct methanol/ethanol fuel cells. The microscopic mechanism of CO oxidation reactions on supported Pt clusters, however, is still unclear and one of the most important issues to be clarified. We investigated the behavior of the Pt_4 clusters on SWNT under CO gas environment. First, we discuss the structural relaxation of Pt_4 clusters on SWNT upon a CO molecule adsorption. Figure 8 shows the structures of Pt_4 cluster on SWNT without CO molecule, structurally fixed Pt_4 clusters with CO molecule, and structurally relaxed Pt_4 clusters with CO molecule, for configurations II and III. Here, it should be mentioned that the structural fluxionality in configuration I is much smaller than that in configurations II and III. Therefore, our discussions are focused on configurations II and III. Although adsorption of CO on the structurally fixed Pt_4 clusters on SWNT gains 2.28 eV for configuration

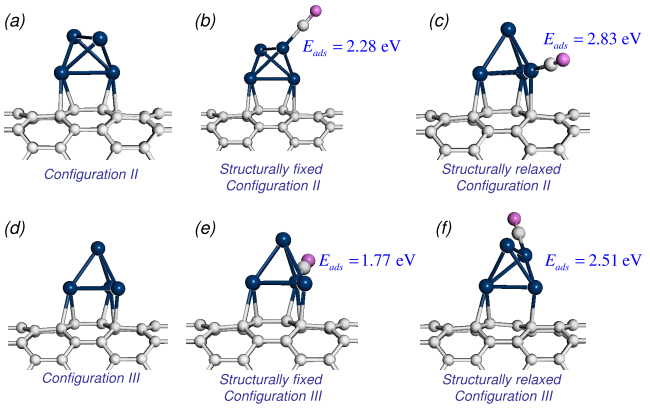

FIG. 8. (Color online) Structures of Pt_4 clusters on (10, 0) SWNT before CO adsorption: (a) configuration II and (d) configuration III. Structures and adsorption energies of CO adsorbed on structural fixed-Pt_4 clusters on (10, 0) SWNT: (b) configuration II and (e) configuration III. Structures and adsorption energies of CO adsorbed on structural relaxed-Pt_4 clusters on (10, 0) SWNT: (c) configuration II and (f) configuration III. The white balls indicate C atoms, the pink (light gray) balls indicate O atoms, and the blue (dark gray) balls indicate Pt atoms.

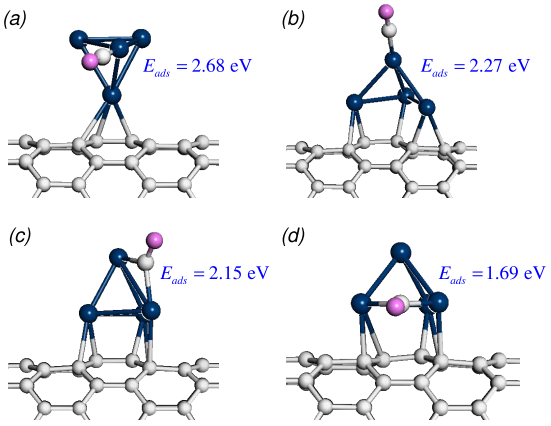

FIG. 9. (Color online) Relaxed structures and adsorption energies of CO on the Pt_4 clusters on (10, 0) SWNT: (a) top site of configuration I, (b) top site of configuration III, and (c)–(d) bridge sites of configuration III. The white balls indicate C atoms, the pink (light gray) balls indicate O atoms, and the blue (dark gray) balls indicate Pt atoms.

II [Fig. 8(b)] and 1.77 eV for configuration III [Fig. 8(e)], these adsorption energies are much smaller than those for relaxed structures, 2.83 eV for configuration II [Fig. 8(c)] and 2.51 eV for configuration III [Fig. 8(f)]. These differences are 0.55 and 0.74 eV. The interesting result is that the Pt_4 cluster on SWNT in configuration II overcomes the barrier of 0.1 eV and converts to the configuration III, whereas the configuration III can overcome a higher barrier of 0.49 eV to convert to the configuration II. Hence, the dynamic structural fluxionality of the Pt_4 clusters on SWNT, a reversible structural change between isomers, occurs under the CO gas environment. The adapting structure of the Pt_4 clusters on SWNT promotes the reaction of adsorbed reactant molecules through the most favorable free-energy path.

Figure 9 shows the relaxed structures of configurations I and III after CO adsorption. The difference in adsorption energy of CO molecule on top sites of configuration I [2.68 eV, Fig. 9(a)] and configuration III [2.27 eV, Fig. 9(b)] is considerably large. In addition, the adsorption of CO molecule also strongly depends on the adsorption sites of the Pt_4 clusters on SWNT. Figures 9(c) and 9(d) show the variation in the adsorption energy of CO molecule on different bridge sites of configuration III from 1.69 to 2.27 eV (variation up to 0.58 eV). The variations can be attributed to the spatial distribution in the charge density and density of states near Fermi level in the supported-Pt_4 clusters, as discussed in Sec. III B. To understand more detailed properties such as reaction rate dynamic structure information will be useful to incorporate into a microkinetic model,[27] because the structural change in the Pt clusters on SWNT will cause a dramatic change in the concentration of active sites of catalyst.

Finally, we carried out electronic-structure analyses to gain insights into the fluxionality of the Pt_4 clusters on SWNT under CO gas environment. Figure 10 shows the PDOS of CO molecule and the *d* PDOS of Pt_4 clusters in on Pt_4 SWNT before and after CO adsorption. There are strong couplings between $2\pi^*$ orbital (lowest unoccupied molecular orbital), 5σ orbital (highest occupied molecular orbital) of

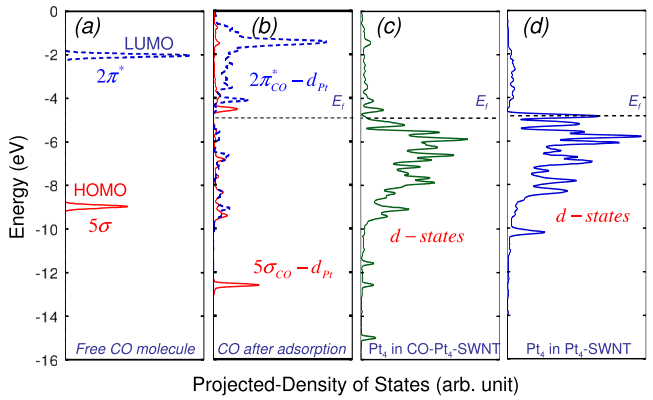

FIG. 10. (Color online) Projected density of states of (a) free CO molecule, (b) CO in the CO-Pt_4-(10, 0) SWNT, (c) *d* states of Pt_4 cluster in the CO-Pt_4-(10, 0) SWNT, and (d) *d* states of Pt_4 cluster in the Pt_4-(10, 0) SWNT. The horizontal dotted lines denote the Fermi levels.

CO molecule and *d* orbitals of Pt cluster, forming a wide range of bonding and antibonding states [Fig. 10(b)]. These couplings cause a significant change in *d*-projected DOS of the supported Pt_4 cluster near Fermi level [Figs. 10(c) and 10(d)]. Our results show that the change in electronic structure via molecular adsorption due to fluxionality and the variation in fluxionality caused by change in electronic structure exhibit a synergistic effect resulting in the wide variety of dynamic reactions of CO molecules with Pt_4 clusters.

In principle, CO molecules can adsorb not only on the Pt clusters but also on the SWNT support. For the pristine SWNT, CO molecules almost do not bind to the surface (ca. 30 meV).[28] However, recent theoretical studies[29,30] have demonstrated that the adsorption energy of CO on the SWNT can significantly improve by deformation of a SWNT or doping impurity of atoms in a SWNT. In addition, our previous study[14] has shown that adsorption of single Pt atoms on SWNT support causes the structural radial deformation of SWNT and the effective charge area on SWNT. Further, we found that the supporting SWNTs mediate interactions between adsorbates. Therefore, the adsorption of Pt clusters on SWNT support is expected to enhance significantly the adsorption of gas molecules such as CO, H_2, O_2, etc. on the SWNT support.

On the other hand, the obtained high-adsorption energies (up to 2.83 eV) of CO molecules on the Pt_4 cluster-SWNT support suggest that the Pt cluster-SWNT system is highly reactive with closed-shell molecules such as alcohols. In addition, CO molecule is one of the main intermediates in the decomposition processes of methanol and ethanol on the Pt catalyst. Many studies[31,32] have shown that the activity of methanol and ethanol decomposition processes on metal surfaces can be predicted from the adsorption energies of intermediates such as CO. Thus, it is expected that the same relations can be applied for Pt clusters-SWNT catalyst. However, detailed and careful investigations are needed to understand the mechanisms of these reactions not only due to the complexity of the reactions, but also due to the unpredicted properties of nanoclusters catalyst.

IV. CONCLUSION

We have investigated the geometry and electronic structure of the Pt_4 clusters on SWNT support using first-principles density functional calculations. We find that the Pt_4 clusters adsorbed on SWNT support exhibit several energetically accessible structural isomers with rather low energy barriers, resulting in the high degree of structural fluxionality. Curvature of SWNT and charge redistribution play important roles in the fluxionality of Pt_4 clusters on SWNT. The high degree of structural fluxionality allows the Pt_4 clusters on SWNT to interact easily with environmental gas molecules such as CO by adapting their structures. Our results show that the change in electronic structure via molecular adsorption due to the structural fluxionality and the variation in structure caused by change in electronic structure exhibit a synergic effect, resulting in the wide variety of dynamic reactions of CO molecules with Pt_4 clusters. These findings provide useful properties of hybrid catalytic structure: metal/CNT. The further investigations are promising to gain insight into catalytic reactivity and to rational design of superior catalysts.

ACKNOWLEDGMENTS

This research was partly supported by the Special Coordination Funds for Promoting Science and Technology commissioned by the MEXT, Japan, by the Special project QGTD.08.09 commissioned by the Vietnam National University-Hanoi, and by Toyota Co., Ltd. The computations presented in this study were performed at the Center for Information Science, Japan Advanced Institute of Science and Technology.

[1] A. T. Bell, Science **299**, 1688 (2003).
[2] F. Raimondi, G. G. Scherer, R. Kotz, and A. Wokaun, Angew. Chem. Int. Ed. **44**, 2190 (2005).
[3] M. Haruta, Chem. Lett. **16**, 405 (1987).
[4] U. Heiz, A. Sanchez, S. Abbet, and W. D. Schneider, J. Am. Chem. Soc. **121**, 3214 (1999).
[5] U. Landman, B. Yoon, C. Zhang, U. Heiz, and M. Arenz, Top. Catal. **44**, 145 (2007).
[6] A. Roudgar and A. Grob, Surf. Sci. **559**, L180 (2004).
[7] M. Valden, X. Lai, and D. W. Goodman, Science **281**, 1647 (1998).
[8] N. Tian, Z. Y. Zhou, S. G. Sun, Y. Ding, and Z. L. Wang, Science **316**, 732 (2007).
[9] H. Hakkinen, S. Abbet, A. Sanchez, U. Heiz, and U. Landman, Angew. Chem. Int. Ed. **42**, 1297 (2003).
[10] D. Astruc, F. Lu, and J. R. Aranzaes, Angew. Chem. Int. Ed. **44**, 7852 (2005).
[11] X. Sun and M. S. Saha, in *PEM Fuel Cell Electrocatalysts and*

Catalyst Layers: Fundamentals and Applications, 1st ed., edited by J. Zhang (Springer, New York, 2008), pp. 655–714.
[12] Y. T. Kim, K. Ohshima, K. Higashimine, T. Uruga, M. Takata, H. Suematsu, and T. Mitani, Angew. Chem. Int. Ed. **45**, 407 (2006).
[13] D. H. Chi, N. T. Cuong, N. A. Tuan, Y. T. Kim, H. T. Bao, T. Mitani, T. Ozaki, and H. Nagao, Chem. Phys. Lett. **432**, 213 (2006).
[14] H. C. Dam, N. T. Cuong, A. Sugiyama, T. Ozaki, A. Fujiwara, T. Mitani, and S. Okada, Phys. Rev. B **79**, 115426 (2009).
[15] P. Hohenberg and W. Kohn, Phys. Rev. **136**, B864 (1964).
[16] W. Kohn and L. J. Sham, Phys. Rev. **140**, A1133 (1965).
[17] B. Delley, J. Chem. Phys. **92**, 508 (1990).
[18] J. P. Perdew, K. Burke, and M. Ernzerhof, Phys. Rev. Lett. **77**, 3865 (1996).
[19] B. Delley, J. Chem. Phys. **113**, 7756 (2000).
[20] H. J. Monkhorst and J. Pack, Phys. Rev. B **13**, 5188 (1976).
[21] E. Durgun, S. Dag, V. M. K. Bagci, O. Gulseren, T. Yildirim, and S. Ciraci, Phys. Rev. B **67**, 201401(R) (2003).
[22] T. A. Halgren and W. N. Lipscomb, Chem. Phys. Lett. **49**, 225 (1977).
[23] N. T. Cuong, A. Fujiwara, T. Mitani, and D. H. Chi, Comput. Mater. Sci. **44**, 163 (2008).
[24] B. Hammer and J. Nørskov, Adv. Catal. **45**, 71 (2000).
[25] B. Hammer, Top. Catal. **37**, 3 (2006).
[26] F. L. Hirshfeld, Theor. Chim. Acta **44**, 129 (1977).
[27] C. V. Ovesen, B. S. Clausen, J. Schiotz, P. Stolze, H. Topsoe, and J. K. Norskov, J. Catal. **168**, 133 (1997).
[28] S. Santucci, S. Picozzi, F. D. Gregorio, L. Lozzi, C. Cantalini, L. Valentini, J. M. Kenny, and B. Delley, J. Chem. Phys. **119**, 10904 (2003).
[29] S. Peng and K. Cho, Nano Lett. **3**, 513 (2003).
[30] L. B. da Silva, S. B. Fagan, and R. Mota, Nano Lett. **4**, 65 (2004).
[31] P. Ferrin, A. U. Nilekar, J. Greeley, M. Mavrikakis, and J. Rossmeisl, Surf. Sci. **602**, 3424 (2008).
[32] P. Ferrin, D. Simonetti, S. Kandoi, E. Kunkes, J. A. Dumesic, J. K. Norskov, and M. Mavrikakis, J. Am. Chem. Soc. **131**, 5809 (2009).